Acta Geodyn. Geomater., Vol. 13, No. 1 (181), 5–18, 2016
DOI: 10.13168/AGG.2015.0046
journal homepage: http://www.irsm.cas.cz/acta

ORIGINAL PAPER

DIFFERENTIATION OF THE ROTATIONAL MOVEMENTS OF THE EUROPEAN CONTINENT'S EARTH CRUST

Kornyliy TRETYAK * and Andriy VOVK

National University Lviv Polytechnic, Institute of Geodesy, Karpinski Street 6, Lviv, Ukraine, 79013

**Corresponding author's e-mail:* kornel@lp.edu.ua

ARTICLE INFO

Article history:
Received 13 May 2015
Accepted 11 September 2015
Available online 21 October 2015

Keywords:
GNSS
The Euler pole
Rotational movements
Tectonic plates

ABSTRACT

This work is devoted to the question of differentiation of the rotational movements of the European continent's Earth crust relative to the Euler pole based on the results of the GNSS observations. Based on the analysis of scientific publications it is determined that with the help of paleotectonic data differentiation of tectonic plates can be performed, that is to allocate separate blocks for whole tectonic plates, which have different rotating characteristics. The methodology and algorithm for conducting tectonic differentiation according to the results of GNSS observations, namely on the basis of vectors of the absolute displacement of GNSS stations are developed. According to the algorithm the division of the European tectonic plates into two blocks with different rotational parameters is obtained. According to certain parameters model values of the velocity vectors of displacement of GNSS stations and their accuracy assessment is calculated. The movement of one block in relation to another as immovable is investigated. The corresponding maps and diagrams to illustrate the obtained results are constructed.

INTRODUCTION

According to the theory of global tectonics, there are major tectonic plates, for which the models, reflecting their movement are developed, its rotational parameters, which are continuously updated are discovered. The boundaries of these plates, as well as models of motion are obtained using the whole set of classical methods of geodesy, geophysics, and other related sciences.

So in the study of tectonic plates, along deep oceanic faults, based on the study of paleotectonic data the displacement of individual blocks of a single tectonic plate is shown, and according to radiocarbon analysis their age can be determined (Fig. 1).

On the basis of the developed paleotectonic data maps it can be seen that the tectonic plates are not solid, but have transverse segments, which move with different angular velocity, resulting in the deposition of rocks of different ages on the ocean's floor along deep oceanic faults. That is, the tectonic plates have cracks and therefore separate blocks which move with different angular velocity are allocated.

However, the manifestation of this fracture is clearly visible only on the bottom of the ocean, on the continent the foundations of tectonic blocks are covered by a sedimentary layer, which hinders the differentiation of tectonic structure of these plates when exploring on land.

The question arises whether it is possible on the basis of GNSS observations to investigate anomalies in the angular velocity of movement of the individual segments of the tectonic plates in the territory of the continents.

THE METHODOLOGY AND ALGORITHM FOR THE TECTONIC PLATES DIFFERENTIATION

Mathematical justification for rotations on the sphere is an Euler's theorem. This theorem says that the general motion of a rigid body with one fixed point is a rotation (Goldstein, 1950). Thus, the movement of rigid plates on a spherical surface of the Earth can be described by simple rotations (Fig. 2).

The connection between the velocity of displacement of the permanent GNSS stations with the coordinates of the Euler pole and angular velocity of rotation in geodetic coordinates can be represented by the following expression (Tretyak and Golybinka, 2006):

$$V_B = \Omega \cdot \cos(\Phi) \cdot \sin(L - \Lambda) \tag{1}$$

$$V_L = \Omega \cdot \begin{pmatrix} \sin(\Phi) \cdot \cos(B) - \\ - \cos(\Phi) \cdot \sin(B) \cdot \cos(L - \Lambda) \end{pmatrix} \tag{2}$$

where Ω – angular velocity of plate's rotation; Φ, Λ – the coordinates of the Euler pole; B, L – the coordinates of the permanent GNSS stations with the determined velocities of displacement in the latitudinal and longitudinal directions V_B, V_L;

For each item of the plurality of permanent stations, nonlinear equations 1 and 2 can be solved. These equations have three unknowns: the coordinates of the Euler pole (Φ, Λ) and angular velocity of plate's rotation (Ω).

Cite this article as: Tretyak K, Vovk A: Differentation of the rotational movements of the European continent´s Earth crust, Acta Geodyn. Geomater. 13 (1) (2016) 5–18. DOI: 10.13168/AGG.2015.0046

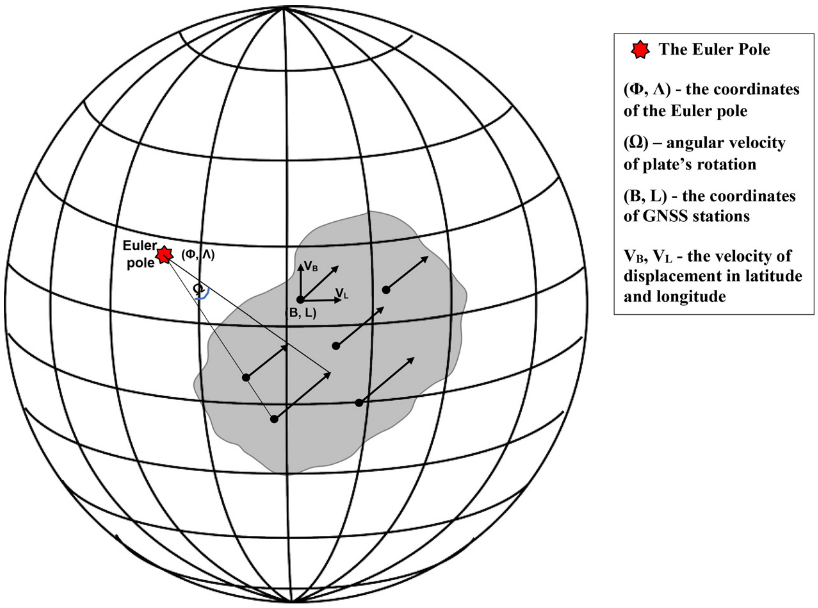

Fig. 2 Motion of tectonic plate around the Euler pole.

Depending on the number of points we will have twice the number of equations, so the number of equations is always greater than the number of unknowns (where n ≥ 2, where n – number of points). Due to this the determination of the unknown parameters (Ω, Φ, Λ) is performed by the least squares method. Having differentiated equations 1 and 2, a linear form of them is presented.

$$\delta_{\Omega}\cdot\left(\frac{dV_B}{d\Omega}\right)-\delta_{\Phi}\cdot\left(\frac{dV_B}{d\Phi}\right)-\delta_{\Lambda}\cdot\left(\frac{dV_B}{d\Lambda}\right)+\left(V_{B_0}-V_{B_i}\right)=v_B \tag{3}$$

$$\delta_{\Omega}\cdot\left(\frac{dV_L}{d\Omega}\right)+\delta_{\Phi}\cdot\left(\frac{dV_L}{d\Phi}\right)-\delta_{\Lambda}\cdot\left(\frac{dV_L}{d\Lambda}\right)+\left(V_{L_0}-V_{L_i}\right)=v_L \tag{4}$$

where: δ_Ω, δ_Φ, δ_Λ – amendments to approximate values of the parameters of the Euler pole (Ω_0, Φ_0, Λ_0); $\frac{dV_B}{d\Omega}$, $\frac{dV_B}{d\Phi}$, $\frac{dV_B}{d\Lambda}$, $\frac{dV_L}{d\Omega}$, $\frac{dV_L}{d\Phi}$, $\frac{dV_L}{d\Lambda}$ - partial derivatives; V_{B0} and V_{L0} – the value of the velocity vector of the absolute horizontal displacement of GNSS stations, computed from approximate values of the parameters of the Euler pole; V_{Bi} and V_{Li} – the estimated values of the velocity vector of the absolute horizontal displacement of GNSS stations in the latitudinal and longitudinal directions.

$$\frac{dV_B}{d\Omega}=\sin(L-\Lambda)\cdot\cos(\Phi) \tag{5}$$

$$\frac{dV_B}{d\Phi}=-\Omega\cdot\sin(L-\Lambda)\cdot\sin(\Phi) \tag{6}$$

$$\frac{dV_B}{d\Lambda}=-\Omega\cdot\cos(L-\Lambda)\cdot\cos(\Phi) \tag{7}$$

$$\frac{dV_L}{d\Omega}=\cos(B)\cdot\sin(\Phi)-\cos(L-\Lambda)\cdot\sin(B)\cdot\cos(\Phi) \tag{8}$$

$$\frac{dV_L}{d\Phi}=\Omega\cdot\left(\cos(B)\cdot\cos(\Phi)+\cos(L-\Lambda)\cdot\sin(B)\cdot\sin(\Phi)\right) \tag{9}$$

$$\frac{dV_L}{d\Lambda}=-\Omega\cdot\sin(L-\Lambda)\cdot\sin(B)\cdot\cos(\Phi) \tag{10}$$

Substituting the derivatives of 5 - 10 in the equation 3, 4, we obtain the equation of the types of amendments 11 and 12.

$$\begin{gathered}\delta_{\Omega}\cdot\left(\sin(L-\Lambda_0)\cdot\sin(\Phi_0)\right)-\delta_{\Phi}\cdot\left(\Omega_0\cdot\sin(L-\Lambda_0)\cdot\sin(\Phi_0)\right)-\\-\delta_{\Lambda}\cdot\left(\Omega_0\cdot\cos(L-\Lambda_0)\cdot\cos(\Phi_0)\right)+\Omega_0\cdot\cos(\Phi_0)\cdot\sin(L-\Lambda_0)-\left(V_{B_0}-V_{B_i}\right)=v_B\end{gathered} \tag{11}$$

$$\begin{gathered}\delta_{\Omega}\cdot\left(\cos(B)\cdot\sin(\Phi_0)-\cos(L-\Lambda_0)\cdot\sin(B)\cdot\cos(\Phi_0)\right)+\\ +\delta_{\Phi}\cdot\left(\Omega_0\cdot\left(\cos(B)\cdot\cos(\Phi_0)+\cos(L-\Lambda_0)\cdot\sin(B)\cdot\sin(\Phi_0)\right)\right)-\\ -\delta_{\Lambda}\cdot\left(\Omega_0\cdot\sin(L-\Lambda_0)\cdot\sin(B)\cdot\cos(\Phi_0)\right)+\\ +\Omega_0\cdot\left(\sin(\Phi_0)\cdot\cos(B)-\cos(\Phi_0)\cdot\sin(B)\cdot\cos(L-\Lambda_0)\right)-\left(V_{L_0}-V_{L_i}\right)=v_L\end{gathered} \quad (12)$$

Using approximate values of the Euler pole's parameters (Ω_0, Φ_0, Λ_0), and the values of amendments (δ_Ω, δ_Φ, δ_Λ), the final values of the Euler pole's parameters are calculated (Ω, Φ, Λ).

$$\Omega = \Omega_0 + \delta_\Omega \quad (13)$$

$$\Phi = \Phi_0 + \delta_\Phi \quad (14)$$

$$\Lambda = \Lambda_0 + \delta_\Lambda \quad (15)$$

With the help of the final parameters, the model displacement velocity of the GNSS stations is being determined. Having obtained an updated parameter values of the Euler pole (Ω, Φ, Λ) their accuracy assessment (m_Ω, m_Φ, m_Λ) is conducted, having calculated already error of unit weight μ.

$$\mu = \sqrt{v^T \cdot \frac{v}{2n-1}} \quad (16)$$

where: v – deviations of the model values of the displacement's velocities of permanent GNSS stations in the latitudinal and longitudinal directions from measured ones;

$$m_\Omega = \mu \cdot \sqrt{Q_{\Omega\Omega}} \quad (17)$$

$$m_\Phi = \mu \cdot \sqrt{Q_{\Phi\Phi}} \quad (18)$$

$$m_\Lambda = \mu \cdot \sqrt{Q_{\Lambda\Lambda}} \quad (19)$$

where: $Q_{\Omega\Omega}$, $Q_{\Phi\Phi}$, $Q_{\Lambda\Lambda}$ – diagonal elements of the correlation matrix.

Since each permanent station is a part of a set of the stations, it has its influence on the final parameters of the Euler pole (Ω, Φ, Λ) and their accuracy, therefore let us analyze the contribution of each station to the accuracy of determining the parameters of the Euler pole for conducting a possible differentiation of tectonic plates. Let's calculate this value Δm_Ω, Δm_Φ, Δm_Λ for each station.

$$\Delta m_\Omega = m_{\Omega i} - m_\Omega \quad (20)$$

$$\Delta m_\Phi = m_{\Phi i} - m_\Phi \quad (21)$$

$$\Delta m_\Delta = m_{\Delta i} - m_\Delta \quad (22)$$

where: m_Ω, m_Φ, m_Λ – root mean square error (RMS) of the parameters of the Euler pole for the entire set of stations; $m_{\Omega i}$, $m_{\Phi i}$, $m_{\Lambda i}$ – root mean square error (RMS) of the parameters of the Euler pole when one station is removed from the set.

Station, for which the values Δm_Ω, Δm_Φ, Δm_Λ are minimal, maximally degrades the accuracy of determining the parameters of the Euler pole. Since the obtained values Δm_Ω, Δm_Φ, Δm_Λ are not the same in dimension, their generalizations are used due to the entropy approach (Tretyak, 1993, 2003). The notion of generalized criterion of changes in the accuracy of the parameters of the Euler pole is introduced. The equation of the generalized criterion of the influence of the removed station (Δm_{gen}) to evaluate the accuracy of the parameters of the Euler pole will be following.

$$\Delta m_{gen} = \ln(\Delta m_\Omega) + \ln(\Delta m_\Phi) + \ln(\Delta m_\Lambda) \quad (23)$$

Therefore, the criterion for assessing the influence of individual station on the definition of the parameters of the Euler pole (Ω, Φ, Λ) and their accuracy is the value Δm_{gen}

The algorithm of differentiation of tectonic plates with rotational parameters is as follows - for each GNSS station the value Δm_{gen} is defined; station, for which the value of Δm_{gen} is minimal, maximally degrades the accuracy of the model values of the rotational parameters; this station is permanently removed from the set of GNSS stations.

For created set of GNSS stations without a station removed in the previous step, similarly the value Δm_{gen} for all other stations is defined. Again station with a minimum value of Δm_{gen} maximally degrades the accuracy of the model, the value of rotational parameters for this sequence and it is also removed from the set. Similarly, by the method of iterations the number of stations that are removed from the set of stations is determined.

For the differentiation of tectonic plates spatial analysis of removed stations and the analysis of changes in the accuracy of their rotational parameters is carried out. Based on this method, the existence of distinction of tectonic plates based on rotating characteristics and which stations belong to its blocks is being determined.

THE RESULTS OF THE DIFFERENTIATION PROCESS OF TECTONIC PLATES

The vectors of the absolute horizontal velocity of displacement of permanent stations in Europe for the period 2000 - 2010, obtained from processing the results of observations of GNSS stations throughout Europe were used as input data for the study of differentiation of tectonic plates of the European continent by rotational parameters. The results of these observations were selected from the database of GNSS measurements of Geodetic Laboratory Nevada NGL *(The Nevada Geodetic Laboratory)*, namely the data of permanent stations, the observations which were carried out not less than 3 years. The locations of the stations used in the study are shown in Figure 3.

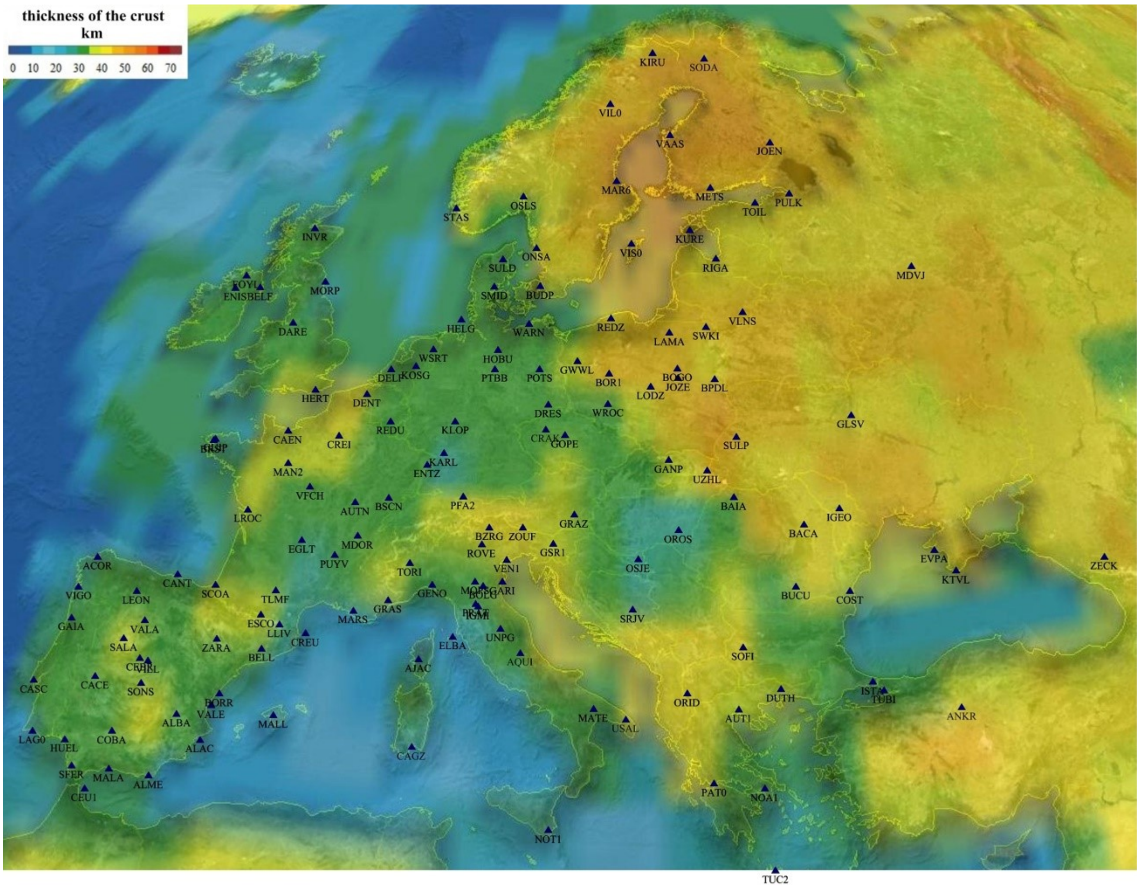

Fig. 3 Scheme of the locations used in the study of permanent European GNSS stations.

Using the results of processed GNSS observations, the directory of the input data, which contains information about GNSS station (name and coordinates) and the value of the horizontal displacements in latitudinal, longitudinal directions (V_B, V_L) was prepared. A fragment of the catalog is listed in Table 1.

Table 1 A fragment of the data directory of permanent GNSS stations used in the study.

name	B, °	L, °	H, m	V_B, mm/year	V_L, mm/year
ACOR	43.364384	-8.398926	67.0	17.6	21.9
AJAC	41.927456	8.762615	99.0	13.0	21.7
ALAC	38.338921	-0.481232	60.0	18.1	28.5
ALBA	38.977917	-1.856415	751.8	13.5	22.0
ALME	36.852535	-2.459442	127.0	14.2	20.1
		...			
ZOUF	46.55722	12.97355	1946.5	14.7	23.9

For approximate values of the parameters of the Rulet pole (Ω_0= 0.257 °/million year; Φ_0 = 58°; Λ_0 = -102°) data from the rotational parameters of the European plate selected from the resource SOPAC (Scripps Orbit and Permanent Array Center) was used. Angular velocity of rotation of the plate (Ω_0) is given in degrees per million years. With the help of the developed methodology, the coordinates of the Euler pole (Φ, Λ), angular velocity (Ω) and accuracy assessment (m_Ω, m_Φ, m_Λ) for the set of all stations (Table 2) were calculated.

The first step was to determine the parameter Δm_{gen} for the entire set of GNSS stations and to determine the station, which corresponds to its minimum value. A fragment of these calculations is shown in Table 3.

At the first stage of iterative procedure, it was determined that the minimum value Δm_{gen} has TUC2 station. This station was removed from the set of all GNSS stations, which gave an improvement for the determination of parameters of Euler poles and their accuracy assessment. Based on a similar iterative

Table 2 Parameters of the Euler pole for the entire set of GNSS stations.

Ω = 0.244±0.009 °/mln. years	Φ = 53.85 ° ± 2.83 °	Λ = –103.88 ° ± 4.49 °

Table 3 A fragment of the results of determining the value Δm_{gen} for the entire set of GNSS stations.

name	Ω, °/mln.y	Φ,°	Λ,°	m_Ω, °/ mln.y	m_Φ,°	m_Λ,°	Δm_{gen}
ZECK	0.244	53.61	-103.87	0.009	2.90	4.55	-14.329
KIRU	0.244	53.64	-103.91	0.009	2.90	4.55	-14.338
CEU1	0.245	53.98	-104.32	0.009	2.85	4.54	-14.342
				...			
TUC2	0.252	55.38	-103.87	0.008	2.29	4.12	-14.717

Table 4 A fragment of serial number of stations removed from the entire set of stations.

name	Ω, °/mln.y	Φ,°	Λ,°	m_Ω, °/ mln.y.	m_Φ,°	m_Λ,°	Δm_{gen}
TUC2	0.252	55.38	-79.69	0.008	2.29	4.12	-14.717
NOA1	0.260	56.90	-83.20	0.007	1.84	3.75	-15.080
PAT0	0.268	58.07	-86.25	0.007	1.45	3.32	-15.521
				...			
MDVJ	0.292	61.92	-85.16	0.001	0.12	0.33	-22.526

procedure, consecutive number of stations that will be taken from the set of all GNSS stations was defined.

The results of determining the number of sequential removal of stations are presented in Table 4.

As Table 4 shows, the removal of stations with a minimum value of Δm_{gen} gives an improvement in determination of parameters of Euler poles and their accuracy assessment.

To illustrate the iterative process the graphs illustrating the change of the parameters of the Euler pole (Ω, Φ, Λ) and accuracy assessment (m_Ω, m_Φ, m_Λ) were built, and a graph of the parameter Δm_{gen} change depending on the number of removed stations k (Figs. 4 - 7) were built.

From Figure 4b, 5b, 6b and 7 a decrease in accuracy of determining the parameters of the pole Euler and generalized parameter Δm_{gen} is shown. In the beginning, the accuracy of determination of parameters increases dramatically, and then this growth is slowed.

For a more detailed analysis of the curve of the generalized parameter Δm_{gen} the gradients of this function $\Delta m_{gen}^{(k)}$ is used. Figure 8 shows the change in the gradients of the function $\Delta m_{gen}^{(k)}$.

Analyzing the change in the gradients of the function $\Delta m_{gen}(k)$ it can be seen that after the first removal of about 10 stations the value of the gradient, by absolute value, sharply decreases. Value of the gradient decreases smoothly to almost zero when reaches up to the 65 - 70 of removed stations. Further removal of stations leads to an increase by absolute value the value of the gradient function $\Delta m_{gen}(k)$.

This suggests that the first 10 stations significantly degrades the accuracy of all rotation models, obviously anomalous velocity vectors are present at these stations. Further removal of the station to the 70 GNSS stations lead to a slow

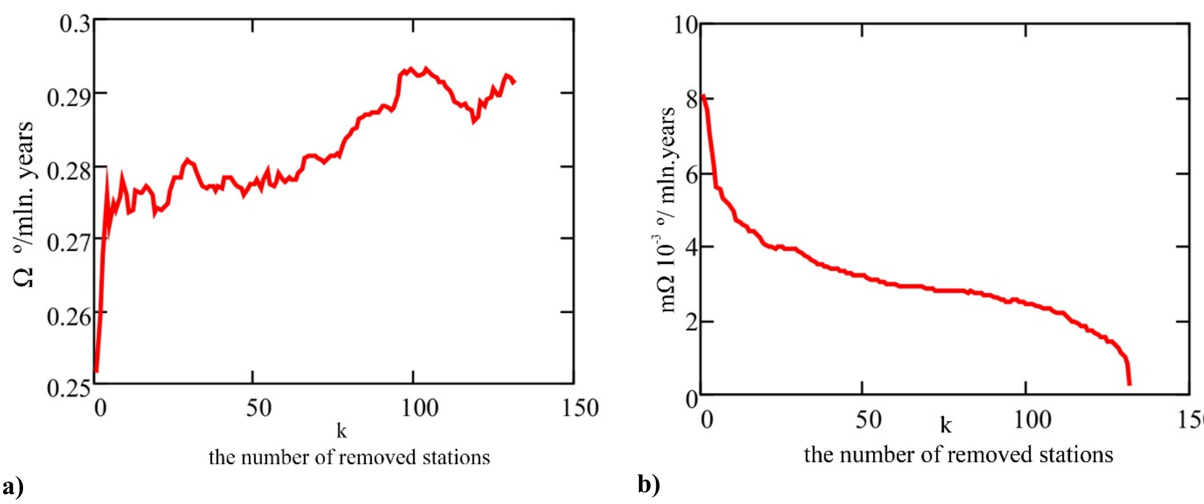

Fig. 4 The change of the angular velocity Ω of rotation of the plate (a) and m_Ω (b) from the amount withdrawn from the set of stations.

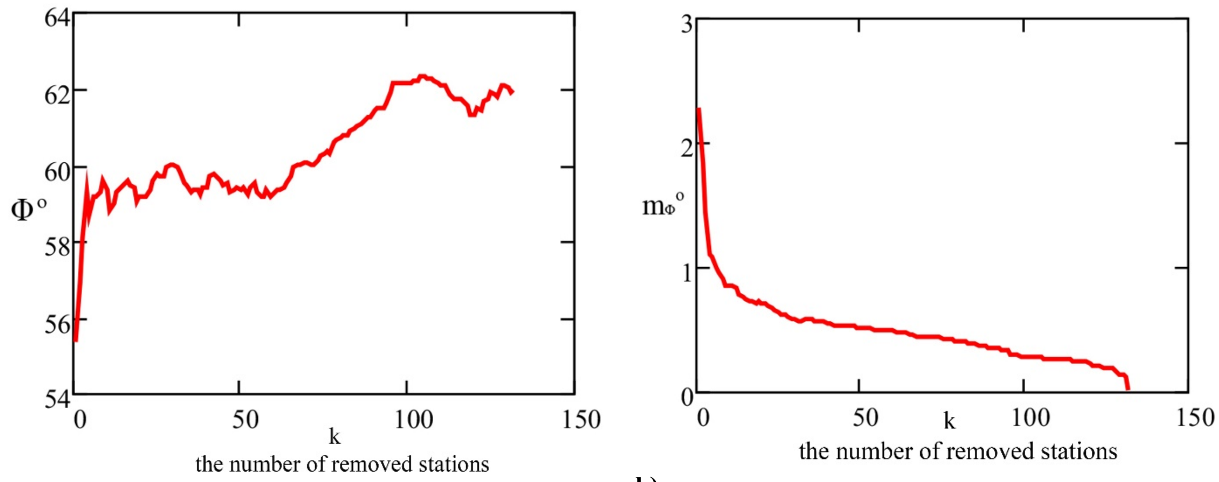

Fig. 5 The change of the latitude Φ of the Euler pole (a) and m_{Φ} (b) from the amount withdrawn from the set of stations.

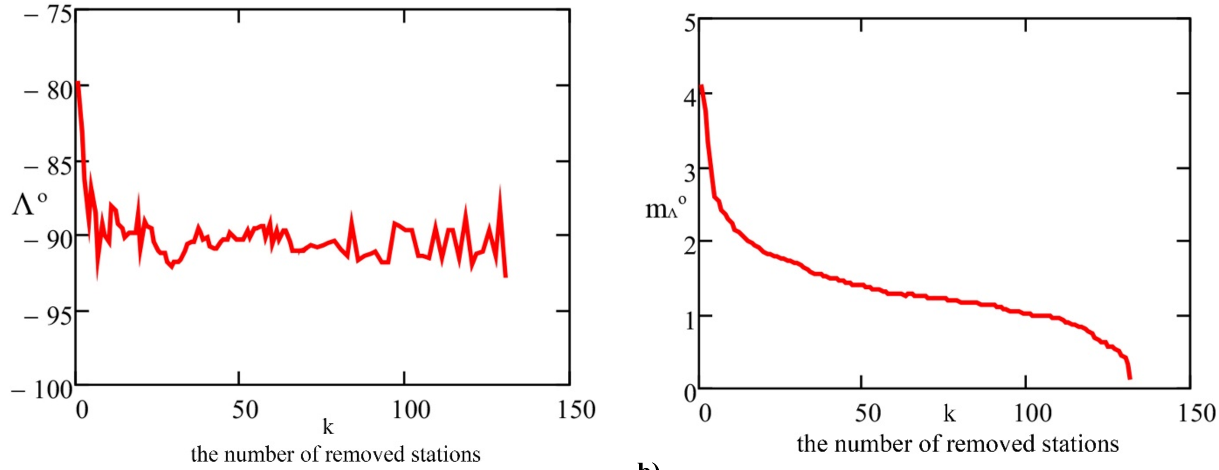

Fig. 6 The change of the longitude Λ of the Euler pole (a) m_{Λ} (b) from the amount withdrawn from the set of stations.

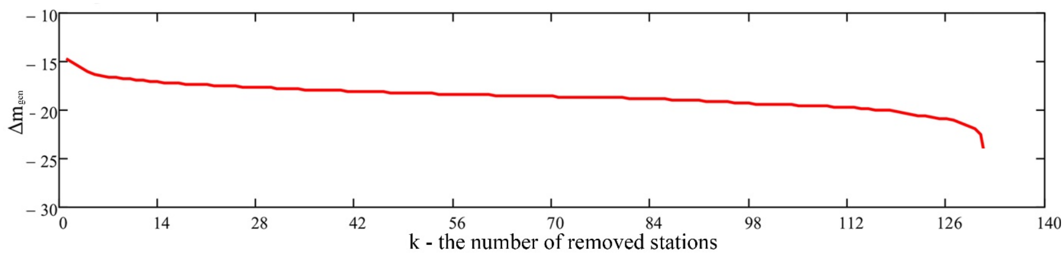

Fig. 7 The change of the generalized parameter Δm_{gen} from amounts withdrawn from the set of stations.

improvement in the accuracy of the model. Withdrawal of the following stations already degrades the accuracy of the rotation model. In this regard, it can be stated that the stations that remain after removal of about 70 stations belong to a homogeneous rotation model. Further removal of the stations of this model leads to deterioration of the accuracy of determining the parameters of the Euler pole.

The use of gradients of the function $\Delta m_{gen}^{(k)}$ is not effective to automate the process of differentiation of tectonic plates by rotational characteristics as a function of gradients $\Delta m_{gen}^{(k)}$ (see Fig. 8) is not smooth.

To automate this process, the curve of the function $\Delta m_{gen}(k)$ is approximated with the help of analytic function that best describes it, instead of gradients the partial derivatives of this function will be used.

Analytically determined that the best approximation for the function $\Delta m_{gen}(k)$ fits the following analytical function.

$$m_{gen}(k) = \frac{a}{b + k^{c}} + d \cdot k^{3} + f \cdot k^{2} \tag{24}$$

where: a, b, c, d, f – constant coefficients of the functions.

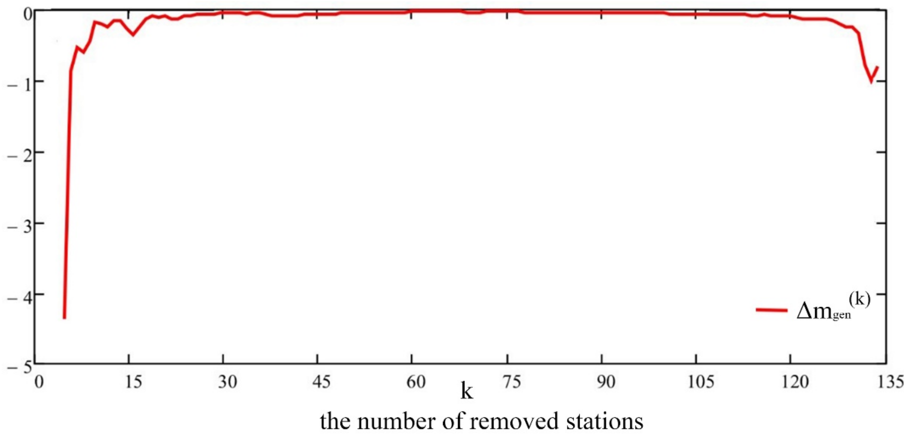

Fig. 8 The change in the gradients of the function $\Delta m_{gen}^{(k)}$.

Having performed an approximation of a function $\Delta m_{gen}(k)$ the values of the unknown coefficients (Table 5) were obtained and a correlation graph between the real and the approximated function $\Delta m_{gen}(k)$ (Fig. 9) was built.

As it can be seen from Figure 9, these functions are almost the same. Let's differentiate function $\Delta m_{gen}(k)_{ap}$ and determine its first derivative $\frac{dm_{gen}}{dk}$.

$$\frac{dm_{gen}}{dk} = 3 \cdot d \cdot k^2 + 2 \cdot k \cdot e - \frac{a \cdot c \cdot k^{c-1}}{\left(b + k^c\right)^2} \quad (25)$$

Figure 10 shows the function of the derivative $\frac{dm_{gen}}{dk}$.

The change in the partial derivative $\frac{dm_{gen}}{dk}$ for the function of the $m_{gen}(k)_{ap}$ is similar to the change of the gradient function $\Delta m_{gen}(k)$ (see Figure 8). It can be also seen that the minimum value of the partial derivative by absolute value appears after the removal of 56 stations from the entire set. The function of partial derivative is smooth, and its use allows efficiently and automatically set the border of the extremum, which corresponds to the limit of stations' removal.

Table 5 The value of the constant coefficients of the function $\Delta m_{gen}(k)$.

Function	Value of the coefficients					Accuracy of approximation
	a	b	c	d	e	
$fm_{gen}(k)$	$4.7 \cdot 10^{-3}$	-0.9	$-1.8 \cdot 10^{-5}$	$-2.9 \cdot 10^{-6}$	$3.3 \cdot 10^{-4}$	1.2 %

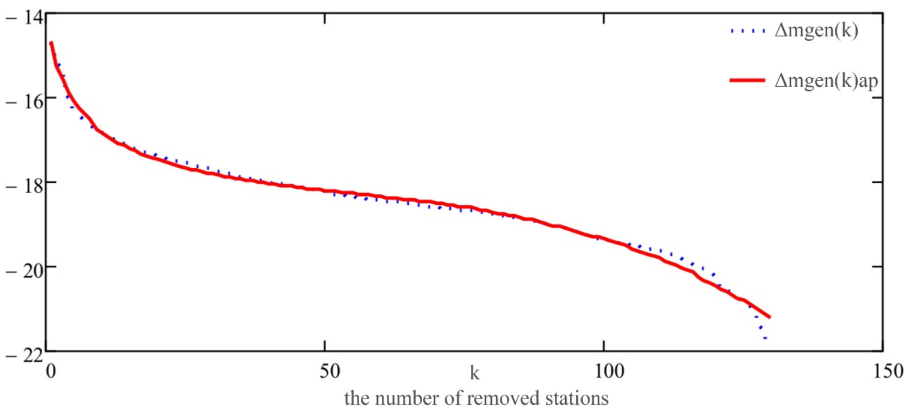

Fig. 9 Function $\Delta m_{gen}(k)$ and function $\Delta m_{gen}(k)_{ap}$.

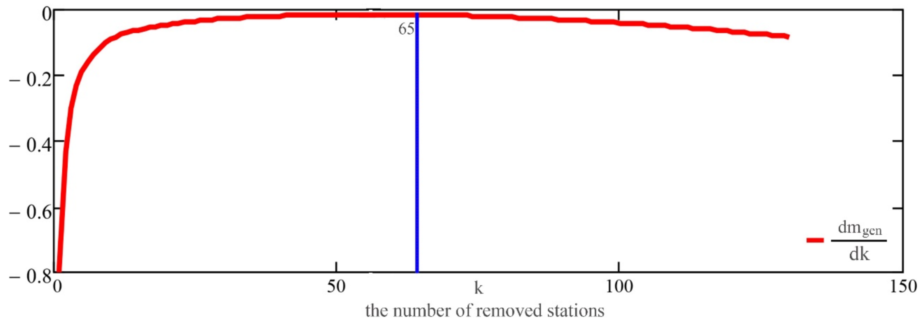

Fig. 10 Function of the derivative $\frac{dm_{gen}}{dk}$.

Table 6 The coefficients of the function $m_\Omega(k)_{ap}$, $m_\Phi(k)_{ap}$ and $m_\Lambda(k)_{ap}$ and the accuracy of approximation.

function	Values of the coefficients					Accuracy of approximation
	a	b	c	d	f	
$fm_\Omega(k)$	$5.1\cdot10^{-4}$	2.6	0.5	$-2.9\cdot10^{-11}$	$3.1\cdot10^{-4}$	2.2 %
$fm_\Phi(k)$	0.02	-0.6	0.2	$-1.8\cdot10^{-9}$	$-9.0\cdot10^{-10}$	1.4 %
$fm_\Lambda(k)$	0.13	-0.8	0.4	$-1.0\cdot10^{-8}$	$1.0\cdot10^{-6}$	1.1 %

The same function approximates the functions $m_\Omega(k)$, $m_\Phi(k)$ and $m_\Lambda(k)$. The results of the determination of the constant coefficients a, b, c, d, and f are presented in Table 6.

Figures 11 – 13 represent graphs of the real ($m_\Omega(k)$, $m_\Phi(k)$ and $m_\Lambda(k)$) and approximated ($m_\Omega(k)_{ap}$, $m_\Phi(k)_{ap}$ and $m_\Lambda(k)_{ap}$) functions.

As it can be seen from Figures 11-13, approximated functions $m_\Omega(k)_{ap}$, $m_\Phi(k)_{ap}$, $m_\Lambda(k)_{ap}$ and functions $m_\Omega(k)$, $m_\Phi(k)$, $m_\Lambda(k)$ are practically identical.

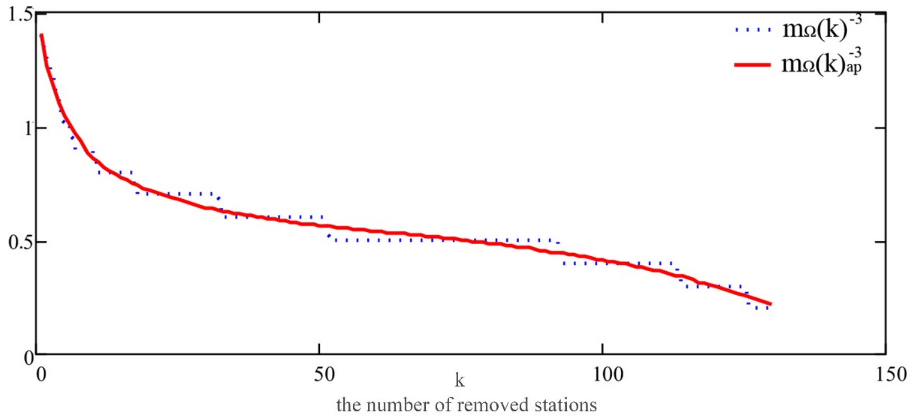

Fig. 11 Function $m_\Omega(k)$ and function $m_\Omega(k)_{ap}$.

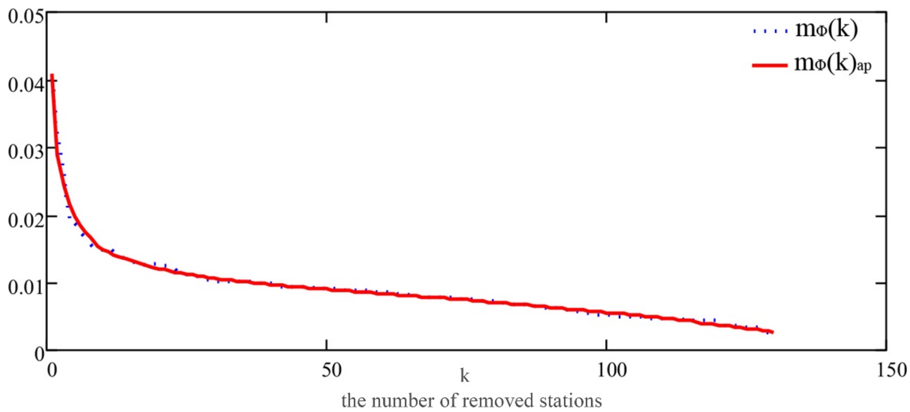

Fig. 12 Function $m_\Phi(k)$ and function $m_\Phi(k)_{ap}$.

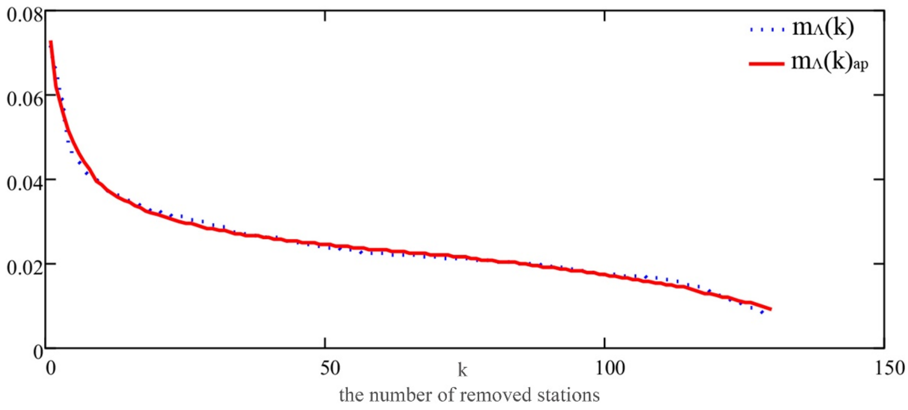

Fig. 13 Function $m_\Lambda(k)$ and function $m_\Lambda(k)_{ap}$.

Figures 14 – 16 demonstrate change the values of partial derivatives for functions $m_\Omega(k)_{ap}$, $m_\Phi(k)_{ap}$, $m_\Lambda(k)_{ap}$.

Figures 14, 15, 16 show the change of the derivatives $\frac{dm_\Omega}{dk}$, $\frac{dm_\Phi}{dk}$, $\frac{dm_\Lambda}{dk}$, and also the enlarged fragments of the curves of these functions in the vicinity of the extremum points for all parameters are shown. The extremums of these functions correspond to 65 - 66 removed from the set of GNSS stations. The change of function of derivatives (see Figs. 14 - 16) almost completely corresponds to the change in the derivative of the function $\Delta m_{gen}(k)$ (see Fig. 10).

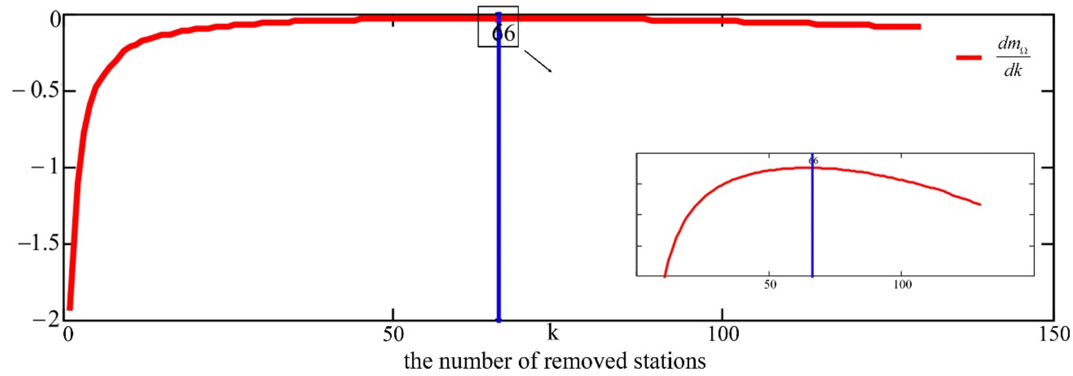

Fig. 14 Function of the derivative $\frac{dm_\Omega}{dk}$.

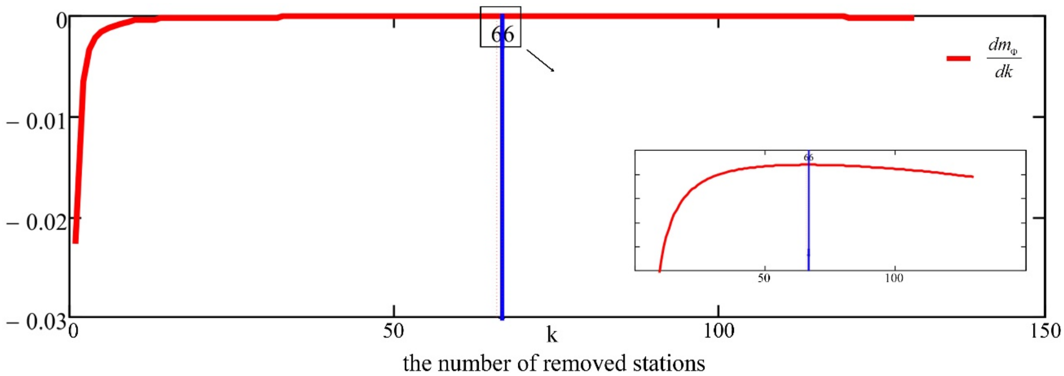

Fig. 15 Function of the derivative $\frac{dm_\Phi}{dk}$.

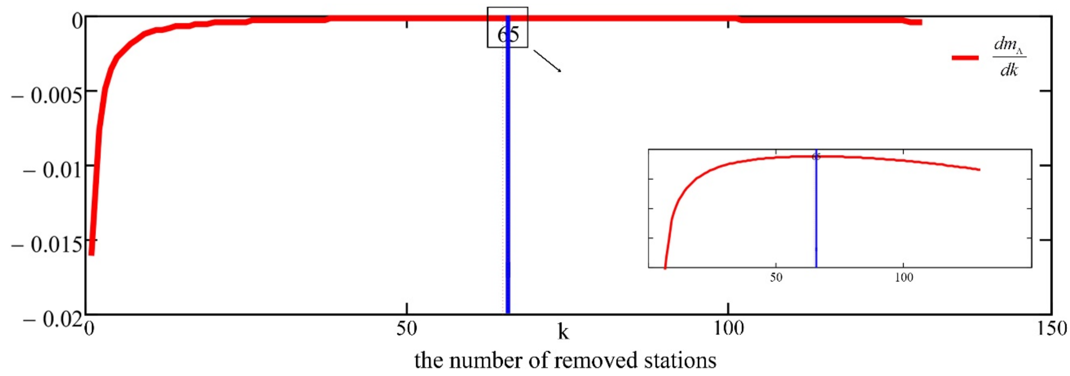

Fig. 16 Function of the derivative $\frac{dm_\Delta}{dk}$.

So, the results of testing the set of stations for all parameters of the Euler pole confirm the need to remove approximately 65 stations from the set of all stations. Eventually, after the withdrawal of these stations, the final set of GNSS stations (the sum of A) with a uniformed rotational parameters, which includes 68 permanent GNSS stations was obtained.

65 of the removed stations form a new set (set B), which similarly can be split into separate groups. For this purpose, similar testing for this set of GNSS stations was conducted with the help of the developed algorithm. Figure 17 presents the change of the generalized criterion of the accuracy of determining the parameters of the Euler pole for this set of GNSS stations.

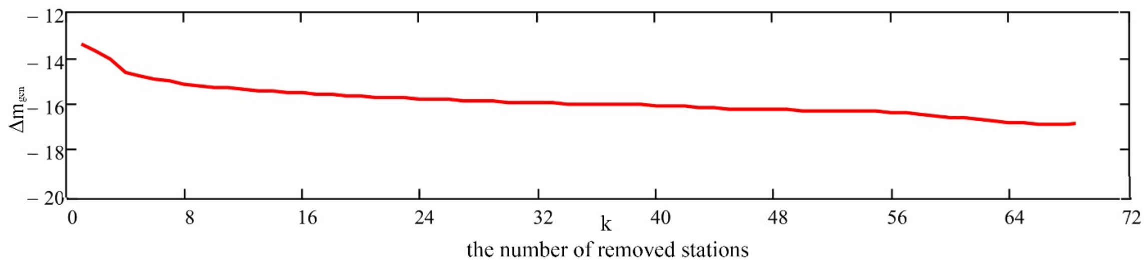

Fig. 17 The change of the generalized accuracy assessment Δm_{gen} for set B.

For a more detailed analysis of the curve of the generalized criterion of accuracy assessment, the gradients of this function were used.

Figure 18 shows the change in the gradients of the function $\Delta m_{gen}(k)$ for set B.

As it can be seen, for this function there is no minimum by absolute value. For a more detailed analysis of the curve change Δm_{gen} for set B, approximation and differentiation of this function was performed. Figure 19 shows the change of the derivative $\frac{dm_{gen}}{dk}$ for set B.

For this function of the derivative there is also no minimum by absolute value, it testifies the impossibility of allocating separate blocks from the set B. Therefore, this set also has its own uniformed rotational characteristics.

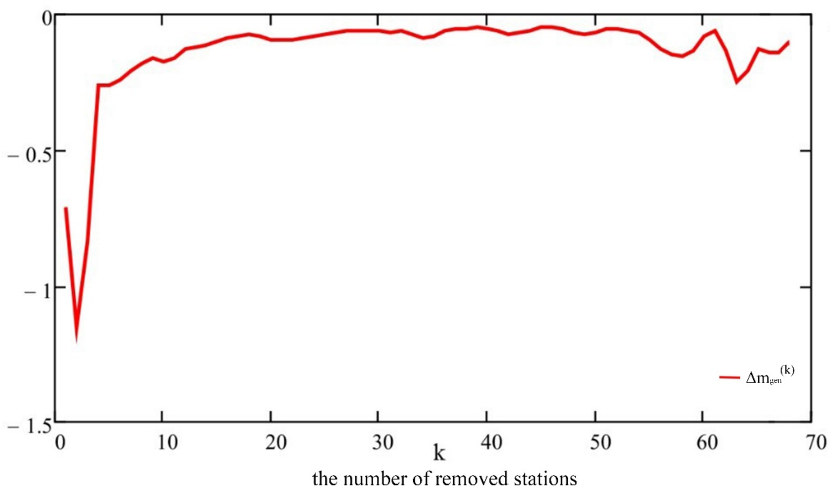

Fig. 18 The change in the gradients of the function $\Delta m_{gen}(k)$ for set B.

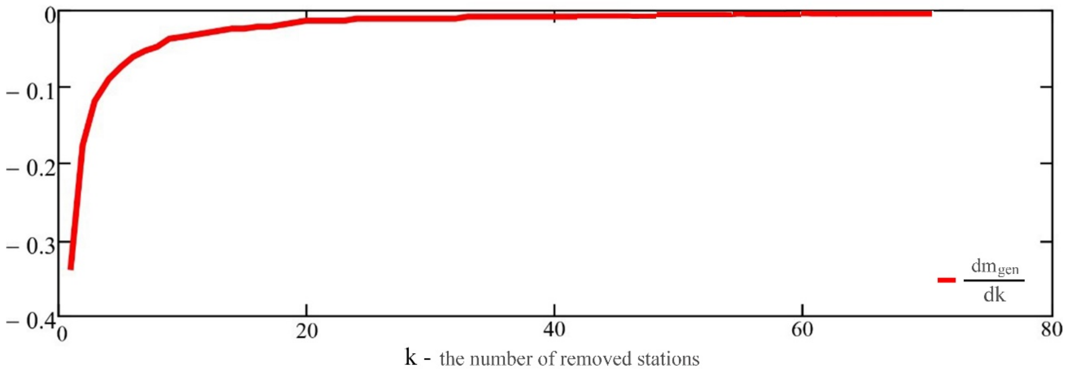

Fig. 19 Function of derivative $\frac{dm_{gen}}{dk}$ for set B.

Figure 20 shows the spatial distribution of sets A and B of permanent GNSS stations with uniformed rotational parameters.

From the figure it can be seen that set A GNSS stations are located in the Northern part of Europe (conditionally North block), and set B stations are located in the Southern part of Europe (conditionally South block).

This distribution confirms that these stations spatially and by kinematic characteristics belong to two different crustal blocks that rotate around their Euler poles that have close location, but different angular velocity (Fig. 21).

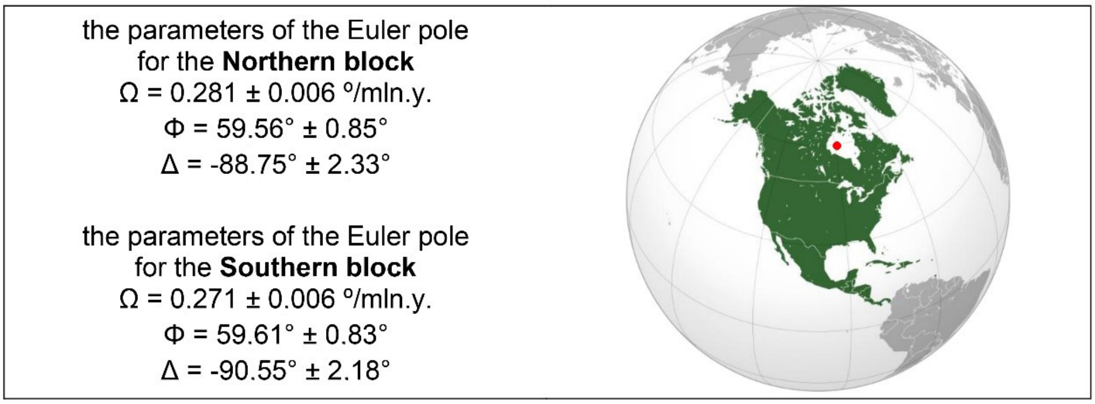

Fig. 21 Parameters and the location of the Euler pole for the Northern and Southern blocks.

The accuracy of determining the angular velocity of rotation of the blocks is the order above its value. The accuracy of determining the coordinates of the Euler pole is within 1º - 2º.

According to certain rotational parameters of the Northern and Southern blocks, for all permanent GNSS stations model horizontal velocity components of the displacement in the latitudinal and longitudinal directions were computed, also the values of deviations of model values from the observed were calculated and accuracy assessment was evaluated.

Figure 22 shows the model horizontal velocity vectors of permanent GNSS stations, defined by the calculated rotational parameters of the two selected blocks.

The North block's vectors are concentrated on the territory of upper Paleozoic folding that exits to the surface and in the areas that are covered by a platform. But the Southern block's vectors are located in the Alpine-Himalayan belt, the areas of Alpine folding in particular, in its main uplifts, in intermountain internal arrays, edge deflections and Neogene basins.

The existence of such division allows making the assumption that between the Northern and Southern blocks there is a border, along which the displacement of the blocks relative to each other is stretched.

To confirm this assumption, the movement of the Northern block in relation to the Southern as immovable was considered, and the map of results was constructed, reflecting this movement (Fig. 23).

Displacement of the entire Northern part of the block occurs in the North-East at a speed of 1.5 mm/year in relation to the static Southern block.

Presence of a single rigid plate of certain segments that move with different angular velocities relative to each other is obtained, also confirmed by the results of tectonic and paleotectonic observations.

A significant displacement of blocks in the mid-Atlantic trench, depicted on the basis of paleotectonic data (Schettino*,* 2001*)* (see Fig. 1), gives a reason to believe that this process lasts for a time of formation of tectonic structures of the European continent.

Conventionally continuing our line of demarcation of the Northern and Southern blocks, its reflection in the data of studies of tectonic boundaries

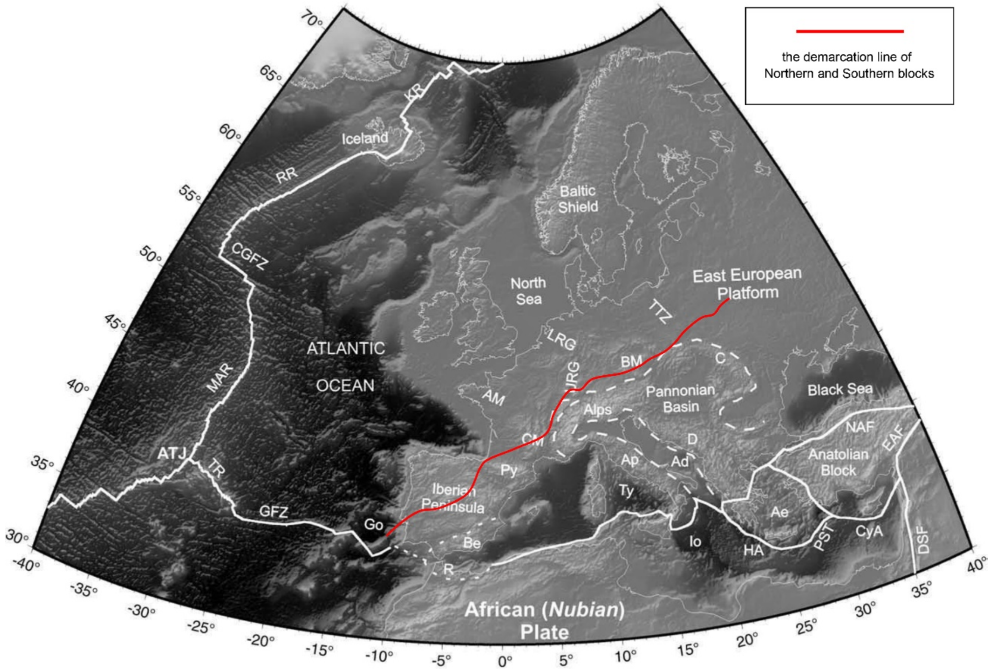

Fig. 24 Simplified tectonic limits of the western Eurasian plate (continuous line) superimposed on topography extracted from ETOPO2 (A.J. Olaiz et. all, 2008) with demarcation line.

in the Western part of the European continent can be seen (Olaiz et. al., 2008) (Fig. 24).

Our results are also consistent with the research results of the European tectonic plates, where certain areas are allocated, Variscan Orogen and Alpine Orogen, the boundaries of which coincide with the border of the Northern and Southern blocks (Plant et. al., 2003).

The developed method allows, with absolute velocities of displacement of the earth's crust, defined with the help of GNSS observations, to conduct the differentiation of the rotational movements of the Earth's crust in relation to the Euler pole.

The research demonstrates the existence in Europe of two tectonic blocks with different rotational characteristics. The boundaries of these blocks are consistent with the data of the paleotectonic research on deep fractions of the Atlantic Ocean.

CONCLUSIONS

On the basis of the developed mathematical apparatus and methods of spatial differentiation of tectonic plates for rotational parameters and results of long-term GNSS observations in Europe the boundaries of two tectonic blocks, which have different rotational parameters (Northern unit: Ω = 0.281 ± 0.006 °/million years, Φ = 59.56° ± 0.85°, Δ = -88.75° ± 2.33°; Southern unit: Ω = 0.271 ± 0.006 °/million years, Φ = 59.61° ± 0.83°, Δ = -90.55° ± 2.18°) are determined.

The movement of these blocks with different angular velocity has reflected on paleotectonic maps of the mid-Atlantic trenches. The boundaries of these blocks coincide with the allocated on the territory of the European continent tectonic structures in particular for the Northern block - Variscan Orogen, for the Southern block - Alpine Orogen.

REFERENCES

Goldstein, H.: 1950, Classical Mechanics. Addison Wesley, Cambridge, MA, 399 pp.

Olaiz, A.J. et al.: 2009, European continuous active tectonic strain-stress map. Techonophysics. DOI: 10.1016/j.tecto.2008.06.023

Plant, J.A., Whittaker, A., Demetriades, A., De Vivo, B. and Lexa, J.: 2003, The geological and tectonic framework of Europe. In: Salminen, R. (ed) Geochemical atlas of Europe. Part 1: background information, methodology and maps. Geological Survey of Finland, Espoo, Finland. http://www.gtk.fi/publ/foregsatlas/article.php?id=4. Cited 28 May 2007

Nevada Geodetic Laboratory [Electronic resource]: NGL. — link: http://geodesy.unr.edu/index.php

Schettino, A. and Scotese, C.R.: 2001, New internet software aids paleomagnetic analysis and plate tectonic reconstructions. Eos Trans., AGU, 82 (45).

Tretyak, K.R.: 1993, Generalized criterion of optimization of geodetic networks. Geodesy, Cartography and Aerial Photography, 55, 93–102, (in Ukrainian).

Tretyak, K.R.: 2003, Posteriori optimization of geodetic networks. Modern geodesic advances of science and industry, 127–141, (in Ukrainian).

Tretyak, K.R. and Golybinka. Y.I.: 2006, Estimation and differentiation movements of a terrestrial surface in Antarctic region. Ukrainian Antarctic Journal, № 4-5, 72–83, (in Ukrainian).

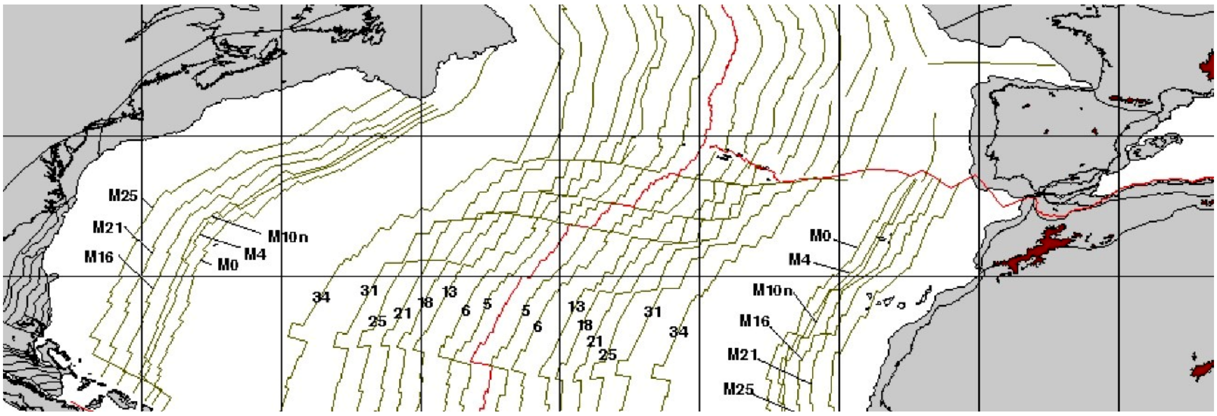

Fig. 1 Isochrons for the Central Atlantic *(*Schettino, 2001*)*.

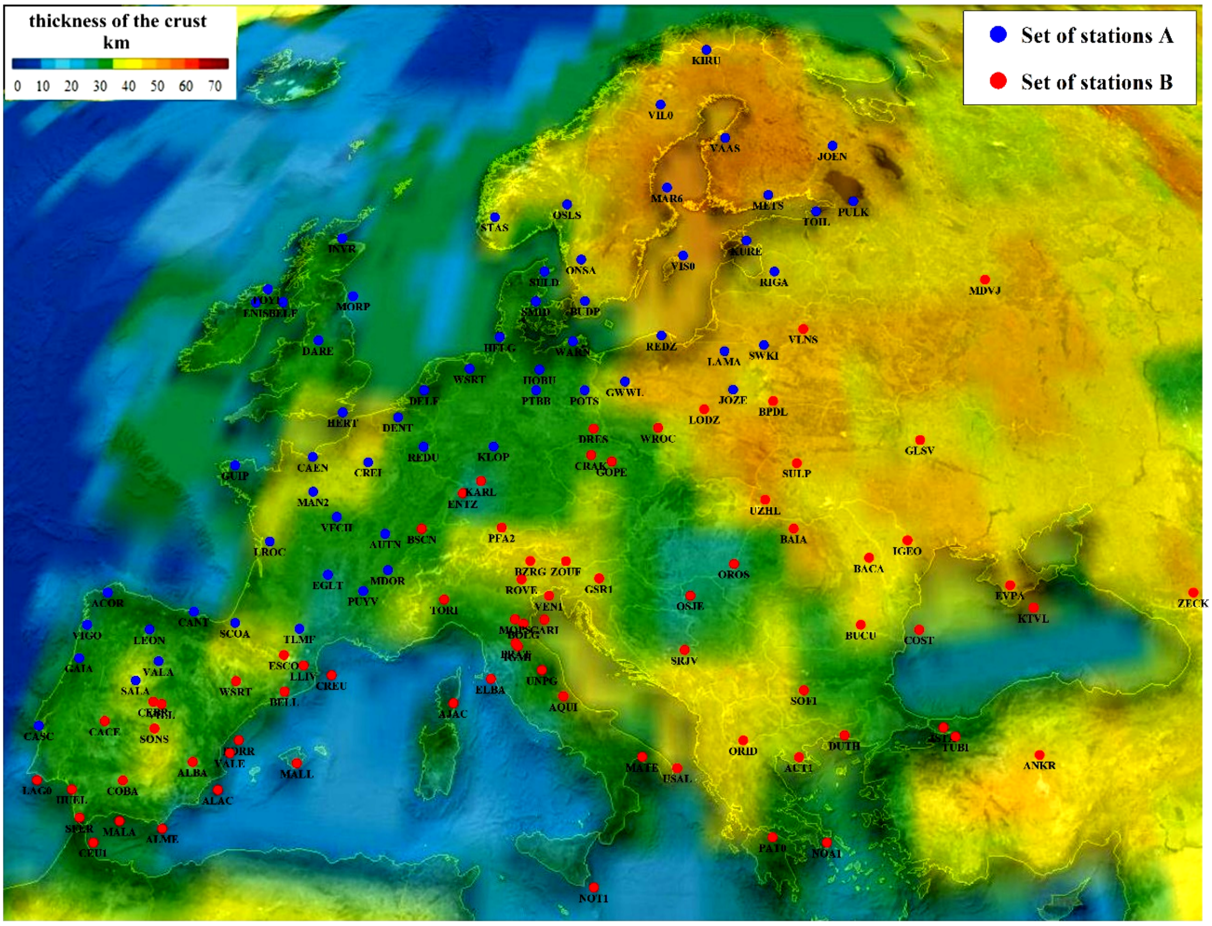

Fig. 20 Sets of GNSS stations A and B.

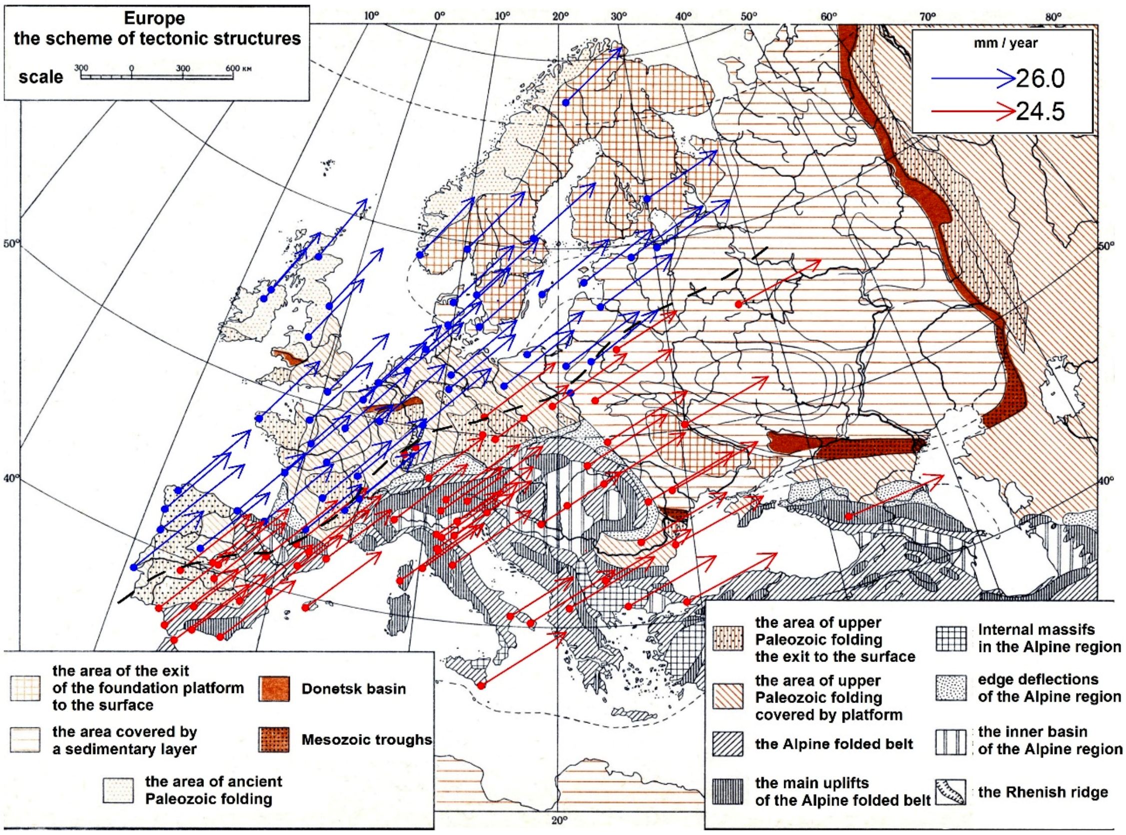

Fig. 22 Scheme of the model horizontal velocity vectors of the Northern and Southern blocks determined by certain rotational parameters.

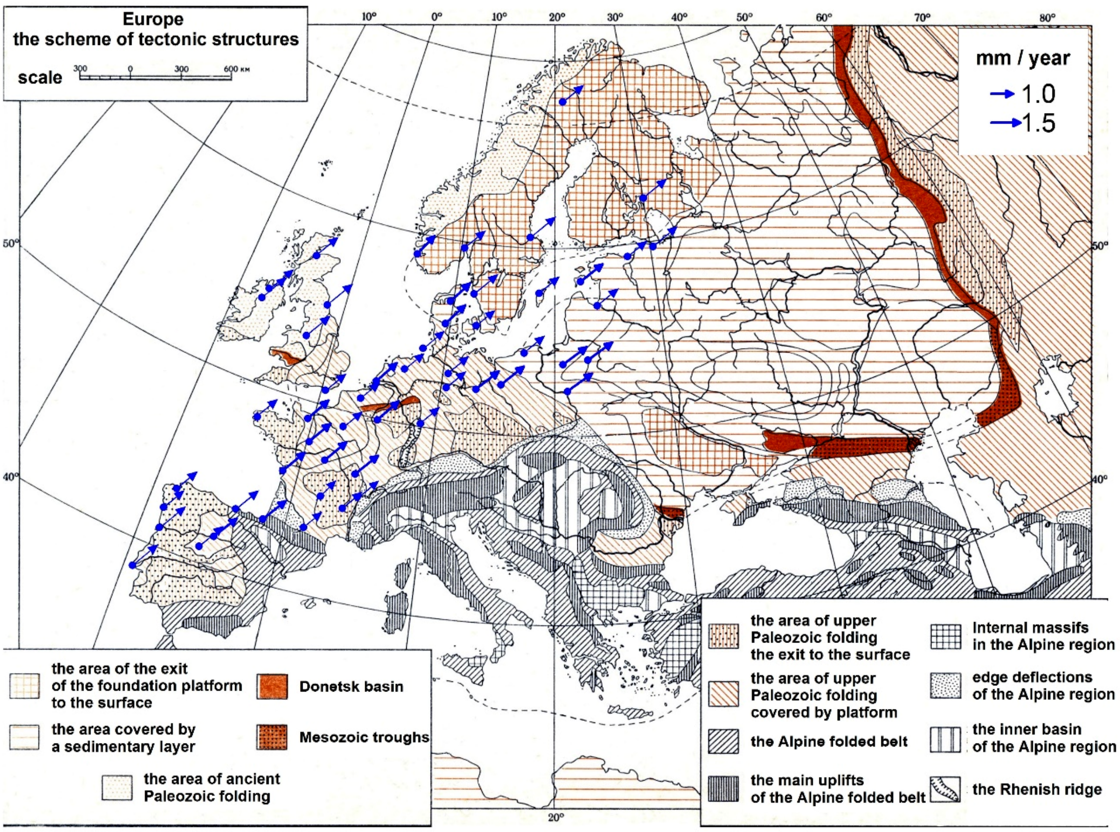

Fig. 23 Scheme of the model horizontal velocity vectors of the Northern block in relation to the Southern (static).